

Applications of TM polarized illumination

Bruce Smith, Jianming Zhou, Peng Xie

Microelectronic Engineering Department, Center for Nanolithography Research, Rochester Institute of Technology, 82 Lomb Memorial Dr., Rochester, New York, 14623

ABSTRACT

The use of transverse electric (TE) polarization has dominated illumination schemes as selective polarization is used for high-NA patterning. The benefits of TE polarization are clear – the interference of diffracted beams remains absolute at oblique angles. Transverse magnetic (TM) polarization is usually considered less desirable as imaging modulation from interference at large angle falls off rapidly as the $1/\cos\theta$. Significant potential remains, however, for the use of TM polarization at large angles when its reflection component is utilized. By controlling the resist/substrate interface reflectivity, high modulation for TM polarization can be maintained for angles up to 90° in the resist. This can potentially impact the design of illumination away from most recent TE-only schemes for oblique imaging angles (high NA). We demonstrate several cases of TM illumination combined with tuned substrate reflectivity for 0.93NA, 1.20NA, and 1.35NA and compare results to TE and unpolarized cases. The goal is to achieve a flat response through polarization at large imaging angles.

An additional application of TM illumination is its potential use for double patterning. As double patterning and double exposure approaches are sought in order to meet the needs of 32nm device generations and beyond, materials and process engineering challenges become prohibitive. We have devised a method for frequency doubling in a single exposure using an unconventional means of polarization selection and by making use of the reflective component produced at the photoresist/substrate interface. In doing so, patterns can be deposited into a photoresist film with double density. As an example, using a projection system numerical aperture of 1.20, with water as an immersion fluid, and a conventional polyacrylate 193nm photoresist, pattern resolution at 20nm half-pitch are obtainable (which is $0.125\lambda/\text{NA}$). The process to transfer this geometry into a hardmask layer uses conventional materials, including the photoresist layer and thin film silicon oxide based materials.

Keywords: TM polarization, hyper NA, TM contrast, polarized illumination

1. INTRODUCTION

Over the past several years, illumination source and photomask optimization has been centered mostly around the use of transverse electric (TE) polarization. The effects of transverse magnetic (TM) polarization has been quite extensively studied and compared to TE polarization¹⁻⁵, but little work has been carried out regarding practical imaging at very large numerical apertures. It is well known that optical behavior of a film stack will influence the reflectivity of incident light with significant dependence on polarization. With application to a photoresist stack, a low level of reflectivity is normally designed below the resist, generally on the order of 1% or less. As angles within the film stack are increased, the disparity between TE and TM polarization increase, requiring either the selective use of a polarized narrow angular bandwidth or a more complex film stack⁶. Where simplicity is normally the goal, a single or dual layer anti-reflective coating is targeted and designed most commonly for TE polarization.

It is also generally well known that while interference between two TE polarized beams is independent of angle, the interference between two TM polarized beams falls off as $1/\cos(\theta)$. This contrast loss in the TM image component would normally prevent its use at angles in the photoresist exceeding 30° (a numerical aperture of 0.85 at a k_1 of 0.25). This analysis assumes only contribution from the incident beams themselves, where any reflected term is suppressed through the use of an anti-reflection layer beneath the photoresist. With a more general consideration of the situation, where reflection is allowed, some insight is gained regarding the “untapped” potential within the TM polarized component. Consider the diagram of Figure 1 which shows how each of two interfering beams produce reflected beams

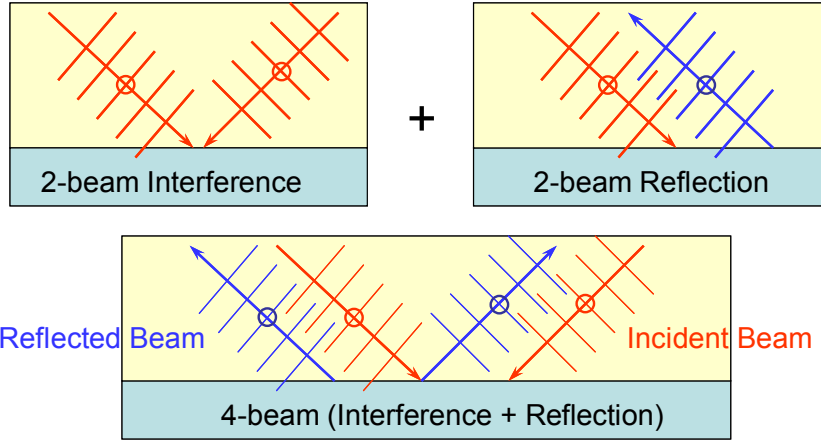


Figure 1. Four beam interference from two incident beams (two transmitting beams and two reflected beams).

from the interface between the propagating media and the substrate. For the TE image component, the resulting electric field in the intersection has only one component along the y direction and can be expressed as:

$$E_{TE} = [(|E_1| + |E_2|)\cos(kx \sin \theta) + i(|E_1| - |E_2|)\sin(kx \sin \theta)]\hat{y} \quad [1]$$

where θ is the incident angle of the beam, k is the wavevector, and E_1 and E_2 are the amplitudes of the electric fields. With TM polarization, the electric field is in the plane of incidence and it has two components along the x and z direction. The resultant electric field is:

$$E_{TM} = [(|E_1| + |E_2|)\cos(kx \sin \theta) + i(|E_1| - |E_2|)\sin(kx \sin \theta)](\cos \theta)\hat{x} + [(|E_1| - |E_2|)\cos(kx \sin \theta) + i(|E_1| + |E_2|)\sin(kx \sin \theta)](\sin \theta)\hat{z} \quad [2]$$

For two-beam interference, typically the two beams have same amplitude and Equations [1] and [2] can be simplified as:

$$E_{TE} = 2|E_1|\cos(kx \sin \theta)\hat{y} \quad \text{and} \quad [3]$$

$$E_{TM} = 2|E_1|\cos(kx \sin \theta)(\cos \theta)\hat{x} + i2|E_1|\sin(kx \sin \theta)(\sin \theta)\hat{z} \quad [4]$$

The resulting intensity images become:

$$I_{TE} = 2|E_1|^2(1 + \cos(2kx \sin \theta)) \quad \text{and} \quad [5]$$

$$I_{TM} = I_{TM_x} + I_{TM_z} = 4|E_1|^2 \cos^2(kx \sin \theta)(\cos^2 \theta) + 4|E_1|^2 \sin^2(kx \sin \theta)(\sin^2 \theta) \quad [6]$$

For an absorbing media, the effective refractive index of the media, n' , is defined where:

$$\frac{\sin \theta_1}{\sin \theta_2'} = n' \quad [7]$$

and intensity image fields for interfering TE and TM polarized beams become ⁴ :

$$I_{TE} = E^2 = 4|A_{TE}|^2 \exp\left(\frac{4\pi k' z}{\lambda_0 \cos \theta_2'}\right) \cos^2(k_0 x NA) = 2|A_{TE}|^2 \exp\left(\frac{4\pi k' z}{\lambda_0 \cos \theta_2'}\right) [1 + \cos(2k_0 x NA)] \quad \text{and} \quad [8]$$

$$I_{TM} = 2|A_{TM}|^2 \exp\left(\frac{4\pi k' z}{\lambda_0 \cos \theta_2'}\right) (1 + \cos(2k_0 x NA) \cos(2\theta_2')) \quad [9]$$

where k' is the effective extinction coefficient of the media (nk/n') and A is the wave amplitude ⁷.

Figure 2 shows experimental results for TM polarized imaging at angles in a photoresist film from 20° to 53° (corresponding to 0.60NA to 1.35NA at $k_1 = 0.25$). Resist SEM images are shown for half pitch features from 80nm to 36nm in thin resist films with BARC layers optimized for reflectivity below 1%. Images were produced with an Amphibian XIS system by varying the numerical aperture across the values depicted. Simulated images are also shown from ILSim⁸. As shown for NA values above 1.20 (corresponding to angles in the resist of 45°), modulation drops to zero and then line/space parity reverse. The results confirm that TM polarization would not be well suited for lithography over a low reflective substrate.

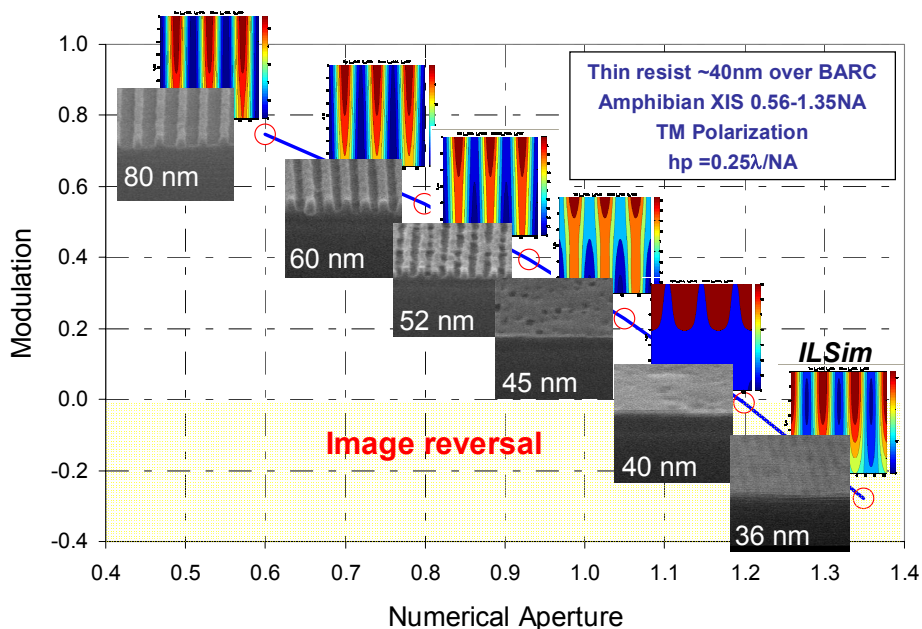


Figure 2. Modulation vs. interference angle (NA) for TM polarized imaging in a thin resist with reflection eliminated. Image reversal occurs as the interfering angle exceeds 45°.

The above analysis shows how the departure of “scalar-like” behavior occurs at relatively low angles in the imaging media. The analysis is, however, limited to an infinitely thick media slab or a film stack which eliminates reflective effects. If an analysis is carried out to include film stack effects, some interesting, and not so intuitive, behavior results. The goal is then to understand the broader impact of polarized illumination, to determine if the contrast loss with TM polarization is necessary, and to identify if such behavior can be taken advantage of.

2. IMAGING WITH A HIGHLY REFLECTIVE SUBSTRATE

Analysis thus far has used the assumption that a standing wave effect is negligible. The root cause of standing wave is identical to two-beam interference. The reflected beam interferes with the incident beam, which results in standing waves along the direction normal to the wafer surface. As Figure 1 shows, a situation with reflection being maximized would be quite different. If E1 and E2 are the two incident waves and they have same polarization state then R1 and R2 are the two reflected waves respectively. E1 with R2 and E2 with R1 will form two pairs of counter-propagating waves if the two incident beams are symmetrical. The amplitude of the reflected beams is comparable with the amplitude of the incident waves when the substrate is highly reflective. The counter-propagating waves will interfere regardless of the polarization state of the incident waves. This results in a four-beam interference situation.

Figure 3 compares TE polarized imaging to TM polarized imaging for three interference angles, 28°, 35°, and 45° over a reflective substrate⁹. The corresponding half-pitch resolution values for these three angles are 60nm, 50nm, and 40nm respectively. For the TE case, the central portion of each plot represents the line regions of the image, which exhibit strong standing waves effects. As expected, the z-nodal spacing increases and the x-nodal spacing decreases with increasing angle. The modulation across x-nodes for the 45° case is approximately 0.86. For the TM case, a strong anti-node develops with increasing angle at the diagonal cross section of z and x nodes. At a 45° angle, these anti-nodes can

possess as much intensity as the nodes, resulting in a spatially averaged modulation of zero between line regions and space regions. If, however, regions are selected which contain just one node, high modulation can be maintained. For example, if the first node is isolated by using a resist with a thickness of:

$$t = \frac{\lambda}{2\sqrt{2}n} \quad , \quad [10]$$

corresponding to a 40nm thickness (assuming a resist refractive index of 1.71, a wavelength of 193nm), the modulation become 0.76, nearly as high as could be achieved using TE polarization.

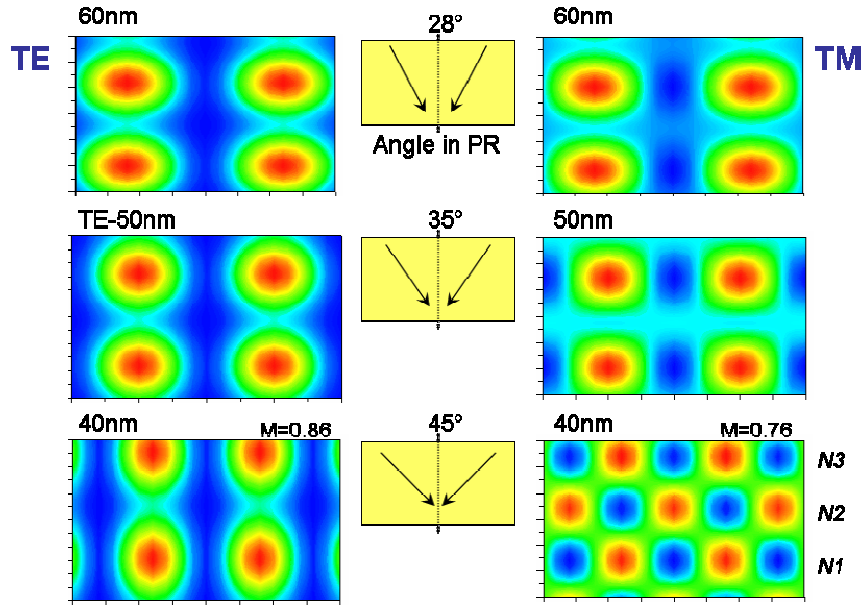


Figure 3. Comparison of interference using TE and TM polarization with a reflective substrate, showing how the intensity at the first node of TM interference can be driven to zero, resulting in high modulation and contrast recovery.

2.1 Analysis of TE and TM cases with reflection

For four-beam interference with TE polarization, the reflected wave can be exactly in-phase or out-of-phase with the incident wave. Assuming the amplitude of the incident wave is E_0 , the sum of the two incident waves is:

$$E_{TE} = |E_{TE0}|e^{-i(kx \sin \theta - kz \cos \theta)} \hat{y} + |E_{TE0}|e^{-i(-kx \sin \theta - kz \cos \theta)} \hat{y} = 2|E_{TE0}| \cos(kx \sin \theta) e^{ikz \cos \theta} \hat{y} \quad . \quad [11]$$

If the reflectivity is r_{TE} at the interface, the sum of the two reflected waves resulting from the incident waves is:

$$R_{TE} = R_1 + R_2 = 2r_{TE}|E_{TE0}| \cos(kx \sin \theta) e^{-ikz \cos \theta} \hat{y} \quad . \quad [12]$$

The total electric field resulting from the incident and reflected waves is:

$$E_{TE \text{ total}} = E_{TE} + R_{TE} = 2|E_{TE0}| (e^{ikz \cos \theta} + r_{TE} e^{-ikz \cos \theta}) \cos(kx \sin \theta) \hat{y} \quad . \quad [13]$$

For four-beam interference with TM polarization, the analysis is more complicated due to the x and z components of the wave. With the z dependent phase factor in the expression, we have the sum of the two incident waves:

$$E_{TM} = 2|E_{TM0}| \left(\cos(kx \sin \theta) (\cos \theta) e^{ikz \cos \theta} \hat{x} - i 2 \sin(kx \sin \theta) (\sin \theta) e^{ikz \cos \theta} \hat{z} \right) \quad [14]$$

where E_{TM0} is the amplitude of the incident wave. The total electric field resulting from the reflected waves becomes:

$$\begin{aligned}
E_{\text{TM}_{\text{total}}} &= E_{\text{TM}} + R_{\text{TM}} \\
&= 2|E_{\text{TM}0}|e^{ikz\cos\theta}(\cos(kx\sin\theta)\cos\theta\hat{x} - i\sin(kx\sin\theta)\sin\theta\hat{z}) \\
&\quad + 2r_{\text{TM}}|E_{\text{TM}0}|e^{-ikz\cos\theta}(-\cos(kx\sin\theta)\cos\theta\hat{x} - i\sin(kx\sin\theta)\sin\theta\hat{z}) \\
&= 2|E_{\text{TM}0}|\left(e^{ikz\cos\theta} - r_{\text{TM}}e^{-ikz\cos\theta}\right)\cos(kx\sin\theta)\cos\theta\hat{x} \\
&\quad - i2|E_{\text{TM}0}|\left(e^{ikz\cos\theta} + r_{\text{TM}}e^{-ikz\cos\theta}\right)\sin(kx\sin\theta)\sin\theta\hat{z}
\end{aligned} \tag{15}$$

As a result, the intensity is a function of both x and z regardless of the polarization state. To see how the contrast lost with TM polarization can be recovered, we can examine a simple case where r_{TM} equals 1 and drop the common term. The electric field can then be written as:

$$E_{\text{TM}_{\text{total}}} = \sin(kz\cos\theta)\cos(kx\sin\theta)\cos\theta\hat{x} - \cos(kz\cos\theta)\sin(kx\sin\theta)\sin\theta\hat{z}. \tag{16}$$

If a value of z is chosen so that $\sin(kz\cos\theta)$ is equal to $\cos(kz\cos\theta)$ are equal, Equations 4 and 15 are similar to each other and the resulting contrast is zero. However, if $\sin(kz\cos\theta)$ is zero and $\cos(kz\cos\theta)$ is unity, Equation 16 becomes similar with Equation 3 and full interference can be achieved. Thus the contrast from TM polarization approaches “scalar-like” behavior and can be recovered, regardless of angle.

2.2 Contrast recovery for TM imaging

To illustrate how modulation of TM imaging can be recovered by high reflection, we consider TM imaging with no reflection, such as that shown in at 1.20NA in Figure 2. The wave propagating angle in the resist is 45° . The two incident waves have electric fields perpendicular to each other, therefore no interference occurs and there is no modulation in this case. As shown above, when the substrate is highly reflective, the contrast can be recovered at certain values of z . If the resist absorbance is neglected for simplicity, Equation 14 can be used to calculate the TM image contrast for various reflection values. The highest contrast that can be achieved with an angle in the resist of 45° is shown in Figure 4. Contrast greater than 90% can be achieved with reflection above 40%. This can be achieved with Al or Si as underlying substrates.

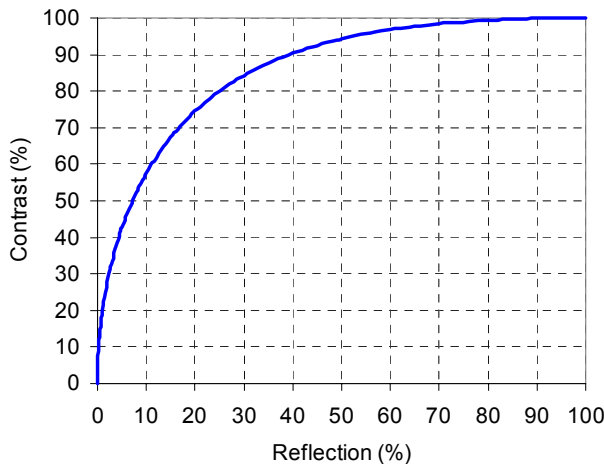


Figure 4. The contrast recovery possible for a 45° interference angle as a function of reflection.

Figure 5 shows simulated results⁹ for 40nm half-pitch imaging using a photoresist with a refractive index of 1.71, a numerical aperture of 1.35, and TM polarized dipole illumination (0.90 center sigma and 0.10 radius sigma). An aluminum substrate is used below a 40nm photoresist layer. Alternative to capturing the first node, imaging of other odd harmonic nodes is also possible using an index matched layer between the resist and the substrate, such as low absorbing dielectric or polymeric film. In this case, the total film stack thickness is 40M nm, where M is an odd integer multiple

representing the number of nodes or harmonics captured. The figure illustrates the latent image in the photoresist and the developed image, which both exhibit image quality comparable to TE cases.

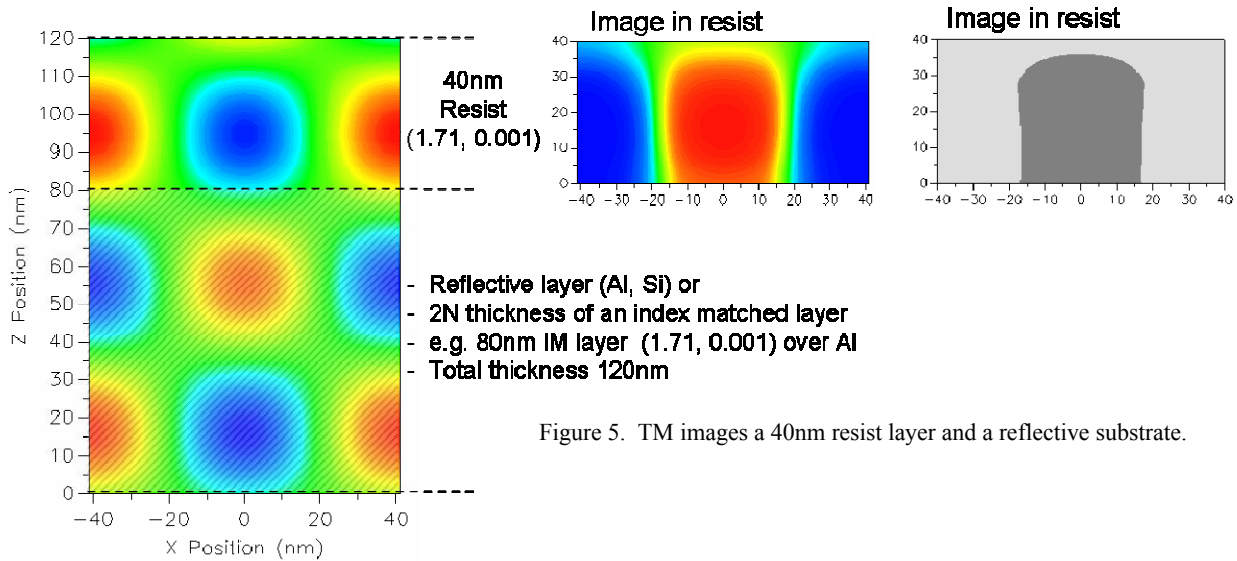


Figure 5. TM images a 40nm resist layer and a reflective substrate.

Figures 6 and 7 are comparisons of modulation and SEM image plots for imaging of 40nm half pitch features in a thin resist layer (JSR ARX2928JN) using an Amphibian XIS system at 1.20 NA (45° in the resist). Figure 6 shows results where reflection is eliminated (using a Brewer Science AR29A BARC), where contrast falls off rapidly as polarization angle changes from 0° (TE) to 90° (TM). Figure 7 shows results where high reflection is utilized by coating the resist over bare silicon (44% reflective), showing a high degree of modulation that is maintained through polarization. In fact, the calculated surface modulation is a conservative measurement, where a higher contrast can be achieved at a depth into the resist film. This may be a more realistic value, which would result in a flatter modulation vs. polarization plot. If the maximum modulation were measure for each case, a value near 1.0 could be maintained throughout.

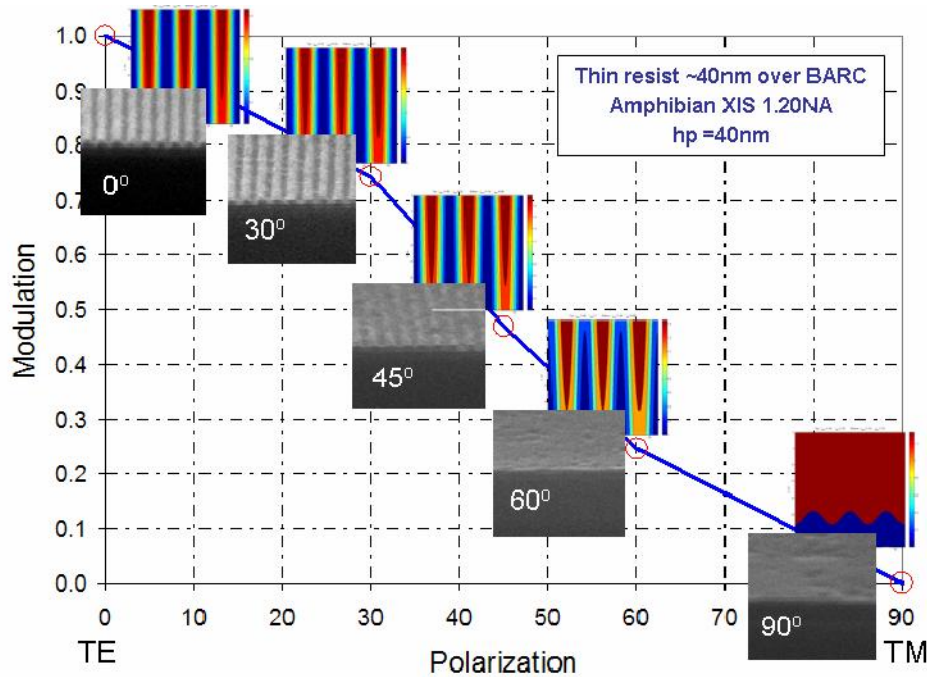


Figure 6. Plot of modulation vs. polarization along with SEM images for 40nm hp imaging with the reflection beneath the photoresist eliminated.

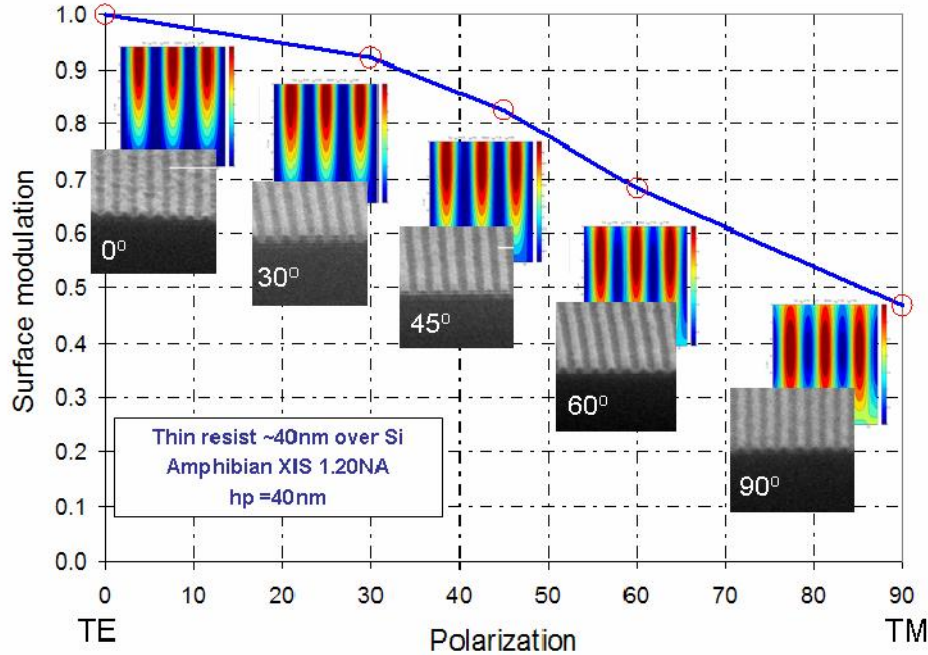


Figure 7. Plot of modulation vs. polarization along with SEM images for 40nm hp imaging with the reflection beneath the photoresist enhanced.

As Figure 4 shows, the influence that substrate reflectivity has to TM image contrast is relatively small as reflectivity values exceed 40%. Figure 8 shows a plot of CD error vs. substrate reflectivity for a resist stack optimized over an aluminum under layer (89% reflective). The error is relatively low for low variations in reflectivity, which can be easily achieved. Figure 9 shows the dose sensitivity to pitch, which has the potential to add variability to the lithography process. This is a direct consequence of the variation in the intensity distribution between nodes and antinodes distributed within the photoresist layer. As shown in Figure 10, there is an ideal resist refractive index based on the targeted pitch that is being imaged, which results in a 45° interference angle in the resist. The ideal refractive index is:

$$n_{PR} = \frac{0.5\lambda}{\sqrt{2}hp} \quad [17]$$

which suggests that a higher refractive index is desirable for smaller geometry when TM or unpolarized illumination is used².

In addition to the imaging examples shown above, series of experiments have been carried out at 0.93NA for 52nm half pitch imaging and 1.35NA for 36nm half pitch imaging. Similar conclusions can be drawn, and the contrast of the TM image state can be recovered using a thin imaging layer over a reflective substrate. Figures 11 and 12 show the results. With regard to the 36nm case, it should be noted that the limitations of the resist are being reached, where a modulation of 0.5 or greater is likely required to be achieve adequate printing of image into resist.

2.3. Applications to unpolarized imaging

One possible application of this method of TM contrast recovery is in the use with an illumination scheme which would not require selective polarization. The advantages would be quite obvious. If unpolarized illumination could be used, decomposition of a mask into x and y components would not be necessary. A single exposure using a cross quadrupole aperture and unpolarized illumination may be possible. Figure 13 shows the simulated results for a TM polarized dipole illuminator (0.90/0.10) and an unpolarized cross quadrupole illuminator of the same settings. The plots show CD variation through focus (for 40nm half pitch) with 6% dose variation for the dipole and 10% dose variation for the cross quad. Although the resist profile for the cross quad is quite shallow, there is significant dose latitude and DOF compared to the TM dipole. Comparatively, no exposure latitude or DOF is possible using a conventional scheme with a BARC layer.

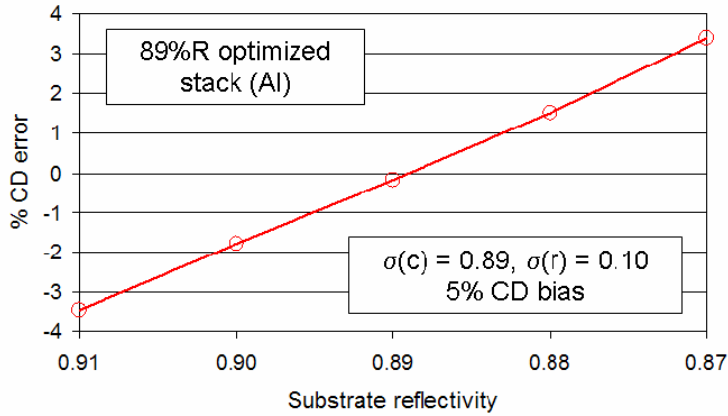


Figure 8. Plot of %CD error vs. substrate reflectivity, showing relative insensitivity to small variations at the resist substrate interface.

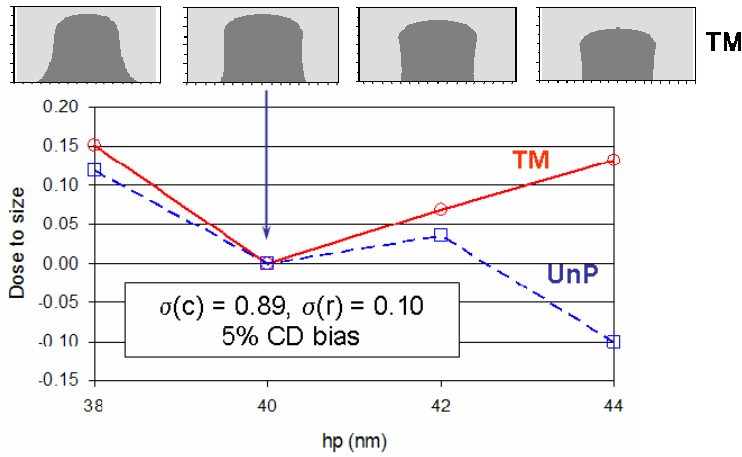


Figure 9. Plot of resist dose to size vs. half pitch, showing the sensitivity of imaging to the interference angle in the photoresist.

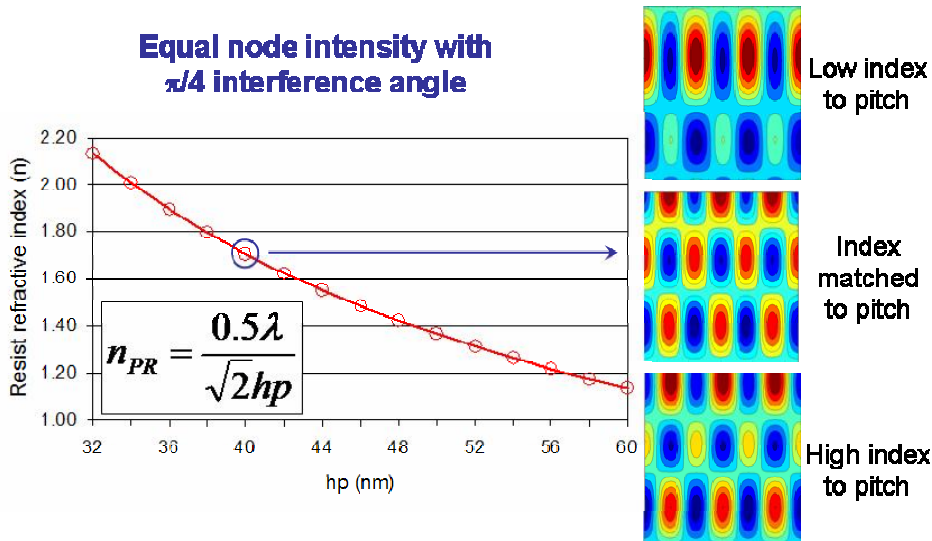


Figure 10. Plot of resist refractive index vs. half pitch, showing how the ideal index is determined when the interference angle is 45° in the resist.

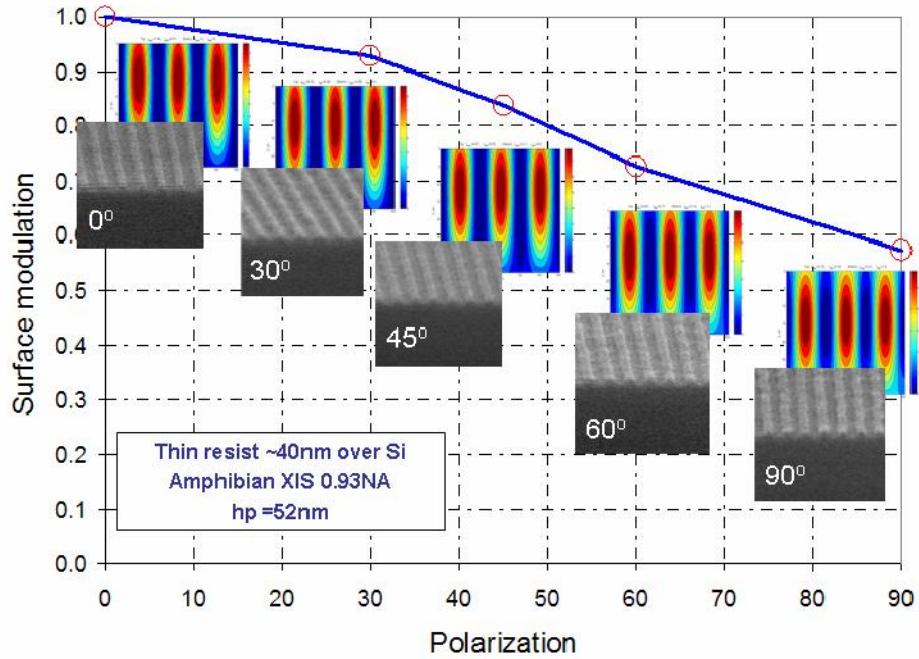


Figure 11. Plot of modulation vs. polarization along with SEM images for 52nm hp imaging with the reflection beneath the photoresist enhanced.

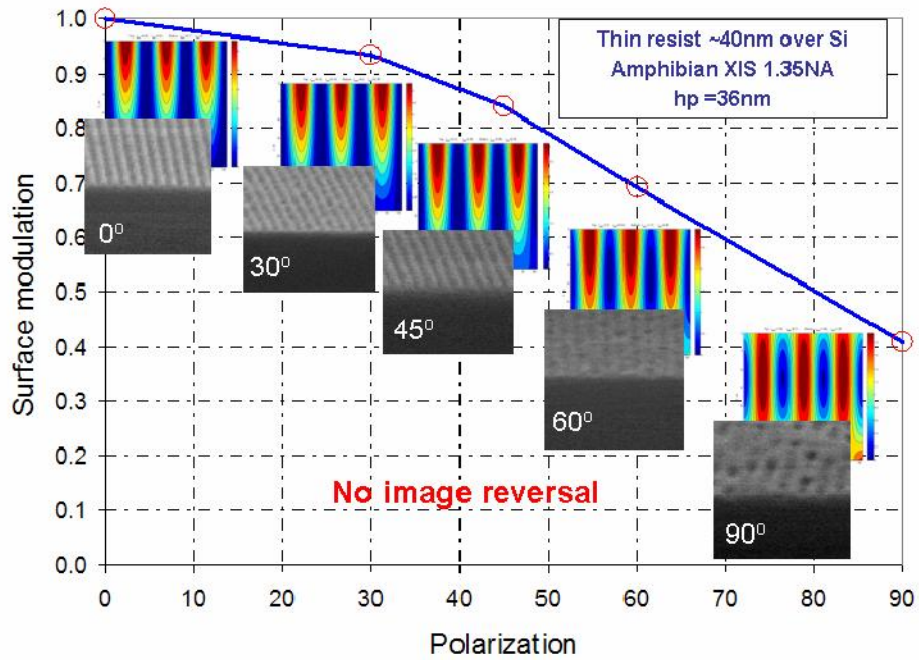


Figure 12. Plot of modulation vs. polarization along with SEM images for 36nm hp imaging with the reflection beneath the photoresist enhanced.

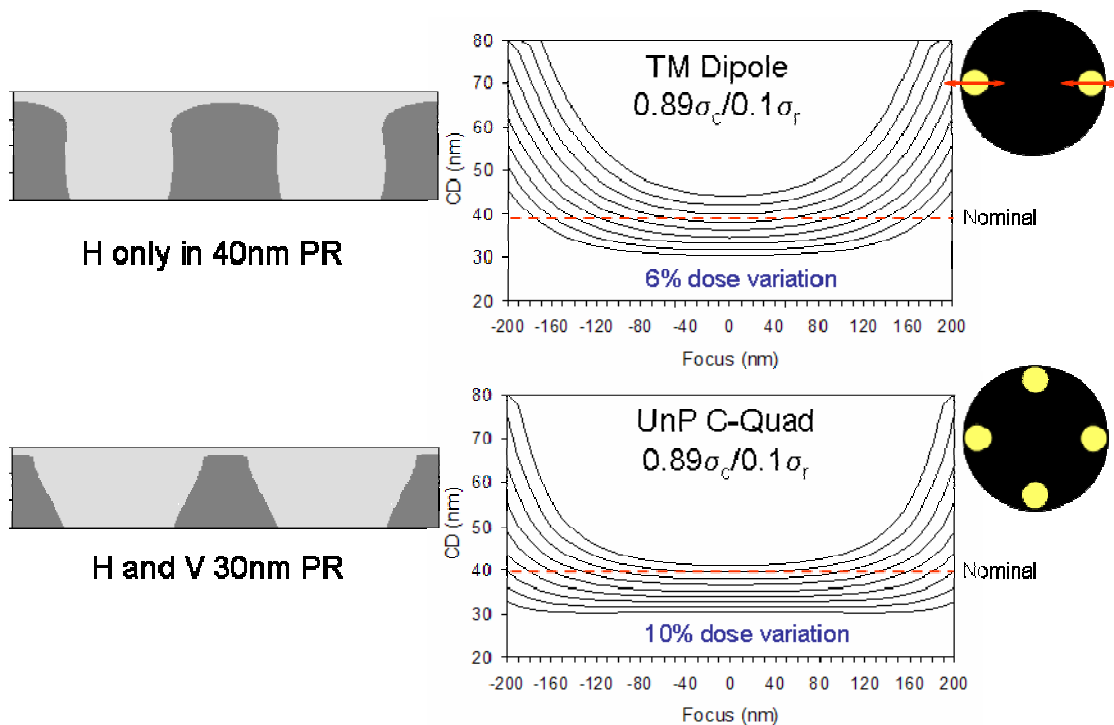


Figure 13. Focus exposure comparisons for TM dipole and unpolarized cross quadrupole illumination using a thin resist over a reflective substrate.

3. APPLICATIONS TO FREQUENCY DOUBLED IMAGING

The creation of interference nodes and anti nodes in a semitransparent film provides opportunities for alternative nanolithography schemes. This may include the imaging of nanospheres or nanorods, as described in an earlier paper⁴. Alternatively, a scheme like that shown in Figures 14 and 15 could be envisioned. By making use of the reflectance present at the interface below a photoresist layer, four-beam interference can result from two incident beams. Through TM polarization, a phase inversion is created, resulting in the deposition of a frequency doubled pattern through the film. By engineering a photoresist stack and processing, a frequency doubled pattern can be projected toward the substrate. Figure 14 shows a stack to take advantage of this concept. A thin imaging layer is coated over an index matched layer, which has beneath it a second photoresist layer and a thick index matched film. The substrate is reflective, as before, using aluminum, silicon, or the like. At a 193nm wavelength, 40nm half-pitch imaging results in an interference angle of 45° in the photoresist (assuming an index of 1.71). Illumination is carried out with a TM polarized dipole, as before. Figure 15 shows the multi-step process that would be carried out to enable both the node and antinode regions to project onto the underlying dielectric layer, providing for a frequency doubled pitch of 40nm (and half-pitch or 20 nm). Challenges include the ability of the second photoresist film to tolerate the processing steps carried out over top of it, as well as the process compatibility of each layer. Index matching is less of a problem as these materials are already currently available. This scheme is an alternative one to the variety of chemistry based double patterning schemes that are being pursued today.

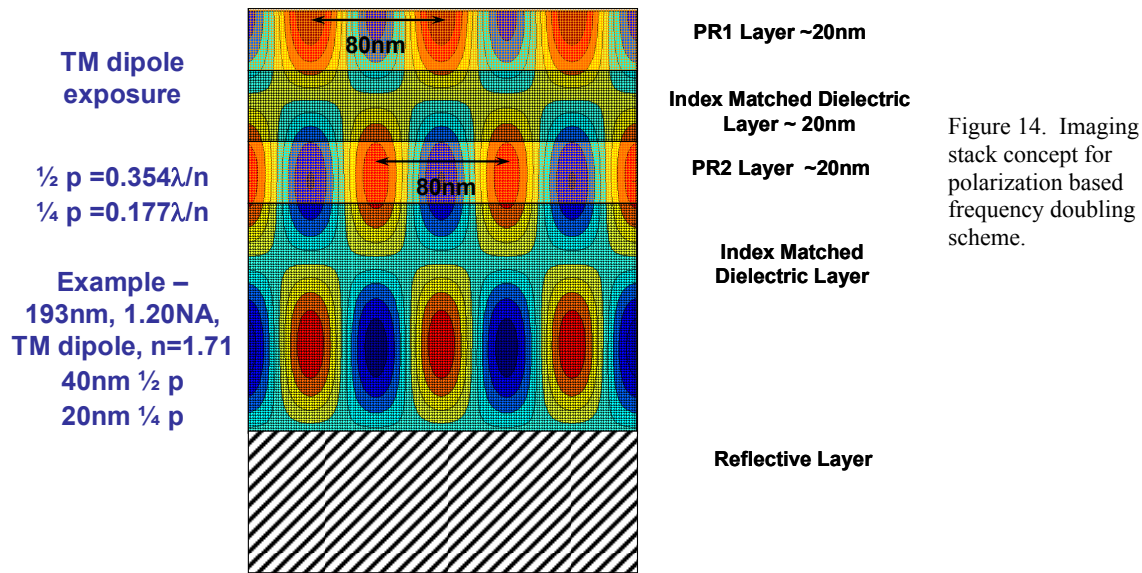


Figure 14. Imaging stack concept for polarization based frequency doubling scheme.

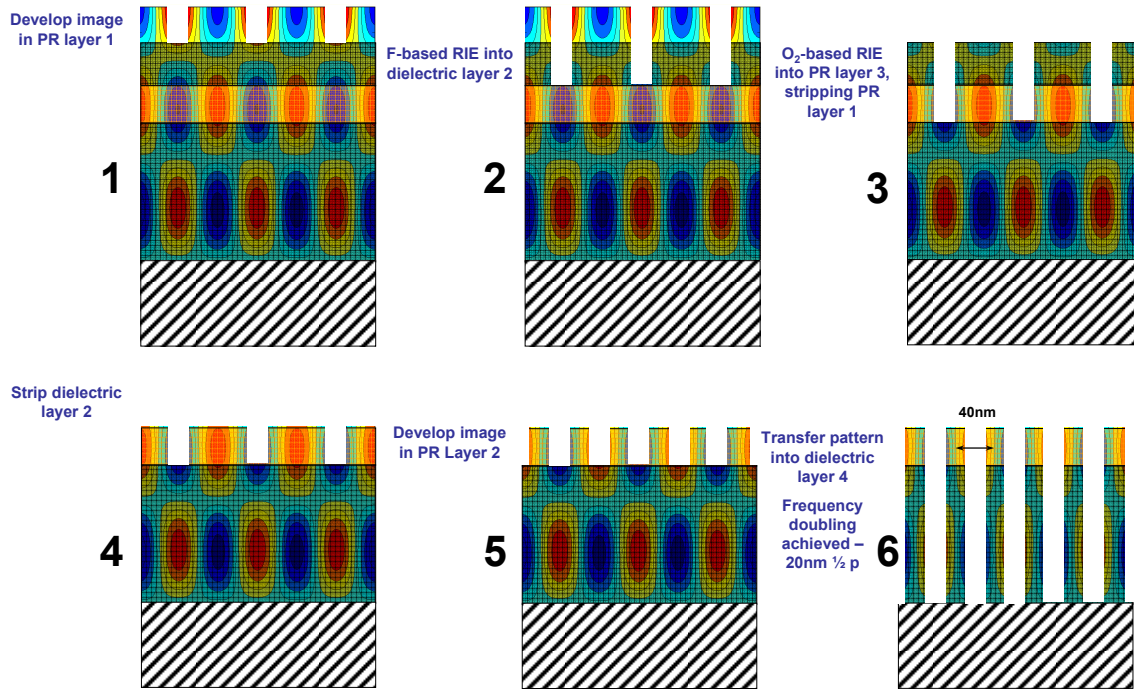


Figure 15. Process sequence concept for polarization based frequency doubling scheme.

4. CONCLUSIONS

We have demonstrated that fundamental imaging with TE and TM polarization is quite different, especially at very large angles. The contrast loss due to TM polarization is not intrinsic and can be recovered to scalar-like behavior in first or odd multiple nodes. Although challenging, an illumination source may not have to be polarized for imaging at high NA. It also follows that high index resists may be desirable for TM and unpolarized imaging. Finally, a frequency

doubling concept using a single exposure has been introduced. The process complexity is not necessarily increased compared to current chemistry based double patterning approaches

5. ACKNOWLEDGEMENTS

The authors gratefully acknowledge the support of the SRC/GRC and Intel Customization Funding, as well as Donis Flagello (ASML), Kafai Lai (IBM), Alan Rosenbluth (IBM), and Yan Borodovsky(Intel).

6. REFERENCES

- [1] Flagello, D.G and Milster, T.D., "Experimental verification of high-numerical aperture effects in photoresist," Proc. SPIE 2197, (1994).
- [2] Smith, B.W., and Cashmore, J., "Challenges in high NA, polarization, and photoresist," Proc. SPIE 4691, (2002).
- [3] Socha, R., Shi, X. LeHoty, D., "Simultaneous source mask optimization (SMO)," Proc. SPIE 5853, (2005).
- [4] Smith, B.W., Zhou, J., "Snell or Fresnel – The influence of material index on hyper NA lithography," Proc. SPIE 6520, (2007).
- [5] Rosenbluth, A., Melville, D., Tian, K., Lai, K., Seong, N., Pfeiffer, D., Colburn, M., "Global optimization of masks, including film stack design to restore TM contrast in high NA TCC's," Proc. SPIE 6520, (2007).
- [6] Smith, B.W., Zavyalova, L., Estroff, A., "Benefitting from polarization – effects of high-NA on imaging," Proc. SPIE 5377, (2004)
- [7] Zhou, J., Lafferty, N., Smith, B.W., Burnett, J., "Immersion lithography with numerical apertures above 2.0 using high index optical materials," Proc. SPIE 6520, (2007).
- [8] Fan, Y., Bourov, A., Zavyalova, L., Zhou, J., Estroff, A., Lafferty, N., "ILSim – A compact simulation tool for interferometric lithography," Proc. SPIE 5754, (2005).
- [9] Prolith/10 KLA/Tencor, (2008).